

1 Measurement report: Exploring the NH<sub>3</sub> behaviors at urban and suburban Beijing:

2 Comparison and implications

3 Ziru Lan<sup>a</sup>, Weili Lin<sup>a</sup>, Weiwei Pu<sup>b</sup>, Zhiqiang Ma<sup>b,c</sup>

4 <sup>a</sup>College of Life and Environmental Sciences, Minzu University of China, Beijing 100081;

5 <sup>b</sup>Environmental Meteorological Forecast Center of Beijing-Tianjin-Hebei, Beijing, 100089, China;

6 <sup>c</sup>Beijing Shangdianzi Regional Atmosphere Watch Station, Beijing, 101507, China

7 Correspondence: Weili Lin ([linwl@muc.edu.cn](mailto:linwl@muc.edu.cn))

8 **ABSTRACT**

9 Ammonia (NH<sub>3</sub>) plays an important role in particulate matter formation, and hence its atmospheric level  
10 is relevant to human health and climate change. Due to different relative distributions of NH<sub>3</sub> sources,  
11 the concentrations of atmospheric NH<sub>3</sub> may behave differently in urban and rural areas. However, few  
12 parallel long-term observations of NH<sub>3</sub> to reveal the different behaviors of the NH<sub>3</sub> concentrations at the  
13 urban and rural sites in a same region. In this study, online ammonia analyzers were used to continuously  
14 observe atmospheric NH<sub>3</sub> concentrations at an urban site and a suburban site in Beijing from January 13,  
15 2018, to January 13, 2019. The observed mixing ratio of NH<sub>3</sub> averaged  $21 \pm 14$  ppb (range: 1.6–133 ppb)  
16 at the urban site and  $22 \pm 15$  ppb (range: 0.8–199 ppb) at the suburban site. The NH<sub>3</sub> mixing ratios at the  
17 urban and suburban sites exhibited similar seasonal variations, with high values in summer and spring  
18 and low values in autumn and winter. The hourly mean NH<sub>3</sub> mixing ratios at the urban site were highly  
19 correlated ( $R = 0.849$ ,  $P < 0.01$ ) with those at the suburban site. However, the average diurnal variations  
20 in the NH<sub>3</sub> mixing ratios at the urban and suburban sites differed significantly, which implies the different  
21 contributions of NH<sub>3</sub> sources and sinks at the urban and suburban sites. In addition to the emission  
22 sources, meteorological factors were closely related to the changes in the NH<sub>3</sub> concentrations. For the  
23 same temperature (relative humidity) at the urban and suburban sites, the NH<sub>3</sub> mixing ratios increased

24 with relative humidity (temperature). Relative humidity was the factor with the strongest influence on  
25 the NH<sub>3</sub> mixing ratio in different seasons at the two sites. The relationships between the NH<sub>3</sub>  
26 concentrations and temperature (relative humidity) varied from season to season and showed differences  
27 between the urban and suburban sites. The reasons for the different relationships need to be investigated  
28 in future studies. Higher wind speed mainly from the northwest sector lowered the NH<sub>3</sub> mixing ratios at  
29 both sites. Similar with other primary pollutants in Beijing, the NH<sub>3</sub> mixing ratios were high under  
30 impacts of air masses from the south sector.

31 **Keywords:** NH<sub>3</sub>; variations; simultaneous observation

32

### 33 **1. Introduction**

34 Ammonia (NH<sub>3</sub>) is the most abundant alkaline trace gas in the atmosphere (Meng et al., 2017). An  
35 excessive NH<sub>3</sub> concentration directly harms the ecosystem; causes water eutrophication and soil  
36 acidification; and leads to forest soil erosion, biodiversity reduction, and carbon uptake variations  
37 (Pearson and Stewart, 1993; Reay et al., 2008; Van Breemen et al., 1983; Erisman et al., 2007). NH<sub>3</sub> can  
38 react with acidic gases to form ammonium salts, which might significantly influence the mass  
39 concentration and composition of particulate matter (Wu et al., 2009). As major components of fine  
40 particle, ammonium salts contribute largely to the scattering of solar radiation and hence influence  
41 climate change (Charlson et al., 1991). Therefore, atmospheric NH<sub>3</sub> is one of the key species relevant to  
42 human health, ecosystem and climate change.

43 After the implementation of policies such as the *12th Five-Year Plan for the Key Regional Air*  
44 *Pollution Prevention and Control in Key Regions* (Ministry of Ecology and Environment of the People's  
45 Republic of China, 2012) and the *Air Pollution Prevention and Control Action Plan* (General Office of  
46 the State Council, PRC, 2013), China, especially the capital city Beijing, has been effectively controlling  
47 the emissions of sulfur dioxide (SO<sub>2</sub>) and nitrogen oxide (NO<sub>x</sub>), which are key precursors of fine particles.  
48 However, the pollution caused by fine particles is still serious (Krotkov et al., 2016; UN Environment,  
49 2019), particularly in winter in the North China Plain, where excess NH<sub>3</sub> promote the haze formation  
50 through heterogeneous reactions (Ge et al., 2019). Studies have indicated that when the SO<sub>2</sub> and NO<sub>x</sub>  
51 concentrations are reduced to a certain extent, reducing NH<sub>3</sub> emissions is the most economical and  
52 effective method to decrease the PM<sub>2.5</sub> concentration (Pinder et al., 2008). In China, the main  
53 anthropogenic sources of NH<sub>3</sub> are livestock and poultry feces (54%) and fertilizer volatilization (33%)  
54 (Huang et al., 2012). Moreover, the atmospheric NH<sub>3</sub> concentration in China has increased with the

55 expansion of agricultural activities, control of SO<sub>2</sub> and NO<sub>x</sub>, and increase in temperature (Warner et al.,  
56 2017). This increase in the NH<sub>3</sub> concentration might weaken the effectiveness of SO<sub>2</sub> and NO<sub>x</sub> emission  
57 control in reducing PM<sub>2.5</sub> pollution (Fu et al., 2017).

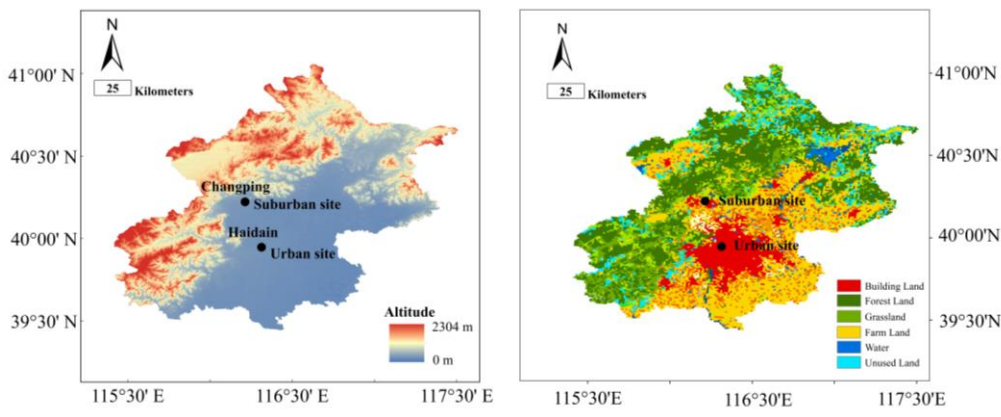
58 The North China Plain is a region with high NH<sub>3</sub> emission (Zhang et al., 2017), and Beijing has one  
59 of the highest NH<sub>3</sub> concentrations in the world (Chang et al., 2016b; Pan et al., 2018). Compared with  
60 studies on pollutants such as SO<sub>2</sub> and NO<sub>x</sub>, considerably fewer studies have been conducted on the NH<sub>3</sub>  
61 concentration in Beijing. Chang et al. (2016a) collected gaseous NH<sub>3</sub> samples during the 2014 APEC  
62 summit (October 18 to November 29, 2014) in the Beijing urban area and concluded that the overall  
63 contributions of traffic, garbage, livestock, and fertilizers to the NH<sub>3</sub> concentration were 20.4%, 25.9%,  
64 24.0%, and 29.7%, respectively. According the data from Huang et al (2012), the NH<sub>3</sub> emissions in  
65 Beijing were from livestock and poultry farming (34.55%), nitrogen-fixing plants (33.57%), fertilizer  
66 use (13.06%), household garbage treatment (8.29%), traffic emissions (5.20%), industrial emissions  
67 (0.14%), biomass combustion (0.42%), and agricultural soil (0.84%). Zhang (2016) measured the NH<sub>3</sub>  
68 concentrations in urban and rural areas of Beijing from January to July 2014 and found that NH<sub>3</sub>  
69 concentration in urban areas was approximately 65% higher than that in rural areas. Meng et al. (2011)  
70 reported that the highest NH<sub>3</sub> concentration in Beijing occurred in summer and the lowest one occurred  
71 in winter, and their results indicated traffic to be a significant source of NH<sub>3</sub> in urban areas. Zhang et al.  
72 (2018) reported the vertical variability of NH<sub>3</sub> in urban Beijing based on one-year passive sampling in  
73 2016/2017 and concluded that local sources such as traffic emissions were important contributors to  
74 urban NH<sub>3</sub>. Meng *et al.* (2020) investigated the significant increase in winter NH<sub>3</sub> and its contribution to  
75 the increasing nitrate in PM<sub>2.5</sub> from 2009 to 2016, and they also concluded that vehicles exhaust was an  
76 important contributor to NH<sub>3</sub> in urban Beijing in winter.

77 Currently, NH<sub>3</sub> is not included in the routine environmental monitoring operation in China. Research  
78 data on NH<sub>3</sub> monitoring, particularly on the synchronous observations of NH<sub>3</sub> concentrations with a high  
79 temporal resolution in urban and suburban areas, are relatively scarce. In this study, high-time-resolution  
80 observations of NH<sub>3</sub> were obtained simultaneously at an urban site and a suburban site in Beijing. The  
81 variation characteristics and influencing factors of the NH<sub>3</sub> concentration were analyzed with  
82 meteorological data to provide a scientific basis for NH<sub>3</sub> pollution control in Beijing.

## 83 2. Materials and methods

### 84 2.1. Measurement sites

85 From January 2018 to January 2019, continuous and simultaneous observations of atmospheric NH<sub>3</sub>  
86 were conducted at an urban site and a suburban site in Beijing. The urban site was located on the roof of  
87 the Science and Technology Building of Minzu University of China (39.95°N, 116.32°E, altitude: 102  
88 m) and the suburban site was in the Changping Meteorological Station (40°13'N, 116°13'E, altitude: 77  
89 m). The suburban site is in the NW direction relative to the urban site and the shortest distance between  
90 these two sites is approximately 32 km (Figure 1). More farm land and glass land are around the suburban  
91 site than the urban site.



92  
93 **Fig. 1.** Location of the observation sites, the topography, and land use of Beijing city.

94

95 2.2. Measurements and data acquisition

96 NH<sub>3</sub> concentrations were measured using two NH<sub>3</sub> analyzers (Ammonia Analyzer-Economical, Los  
97 Gatos Research Inc., USA), which have the minimum detection limit of <0.2 ppb and the maximum drift  
98 of 0.2 ppb/24hrs. The NH<sub>3</sub> analyzers were deployed in air-conditioning rooms. These analyzers use off-  
99 axis integrated cavity output spectroscopy (OA-ICOS) technology, which is a fourth-generation cavity-  
100 enhanced absorption technique, to simultaneously measure NH<sub>3</sub> and water vapor (H<sub>2</sub>O) in the atmosphere.  
101 The incident laser beam of the OA-ICOS technology deviates from the optical axis, which differs from  
102 the traditional coaxial incidence mode. The axial incidence mode of the OA-ICOS technology can  
103 increase the optical path, stimulate additional high-order transverse modes, effectively suppress the noise  
104 of the cavity mode, reduce the cross interferences and errors due to contaminants existing in the cavity,  
105 and improve the detection sensitivity (Baer *et al.*, 2002; Baer *et al.*, 2012). The analyzer method is a  
106 quasi-absolute measurement, which theoretically does not require calibration. However, to ensure the  
107 comparability of the obtained data with other monitoring data, NH<sub>3</sub> standard gas (Beijing AP BAIF Gases  
108 Industry Co., Ltd.) was used for comparison measurement before the observation. The recorded  
109 concentrations were revised with respect to the reference NH<sub>3</sub> concentration in the standard gas mixture.

110 Ambient air was drained at >0.4 L/min through Teflon lines (1/4"OD) from a manifold. The lengths  
111 of the Teflon lines were designed as short as possible (less than 2 m from the manifold). Particulate  
112 matters were filtered by Teflon membranes with a pore size less than 5 μm. Since NH<sub>3</sub> easily "sticks" to  
113 surfaces (like inside walls of tubes), heated sample lines were suggested by many measurement studies.  
114 However, according our test (Fig. S1) in the lab, when heating (70°C) was on, there did have a peak  
115 lasting 5–6 min minutes and then decreasing to the normal levels in ambient air, which means a new  
116 balancing process has been established in less than 10 min. This suggests that heating is not necessarily

117 a solution for NH<sub>3</sub> sticking. Keeping the relatively stable balance between adsorption and desorption of  
118 NH<sub>3</sub> in the sampling system is important. When tested using air of different humidity, only very sharply  
119 changes of humidity obviously influenced and changed the balance, and a new balance needed tens of  
120 minutes to reestablished (Fig. S2). Under the normal weather conditions, humidity changes in a relatively  
121 smoothing way unless a quickly changing weather system, like rain, is approaching. The minute-level  
122 data were converted into hourly averages in the data analysis process and the hourly resolution can  
123 smooth the effect to some extent caused by variations in humidity and temperature during the observation.

124 The balancing idea was also used to carry out multi-point calibrations on NH<sub>3</sub> analyzers (Fig. S3).  
125 A high mixing ratio (e.g. 400 ppb or higher) of NH<sub>3</sub> mixing gases were firstly produced by a dynamic  
126 diluter and measured by the NH<sub>3</sub> analyzers overnight. After the signals reached the stable level, other  
127 lower span values were switched in turn. At each span point, the measurement time was lasting at least  
128 40 minutes or longer. Then a linear regression function was obtained with R<sup>2</sup> higher than 0.999.  
129 Nowadays, NH<sub>3</sub> in compressed gas cylinder is also trustworthy, as confirmed by the comparison with the  
130 NH<sub>3</sub> standard in a permeation tube (Fig. S4).

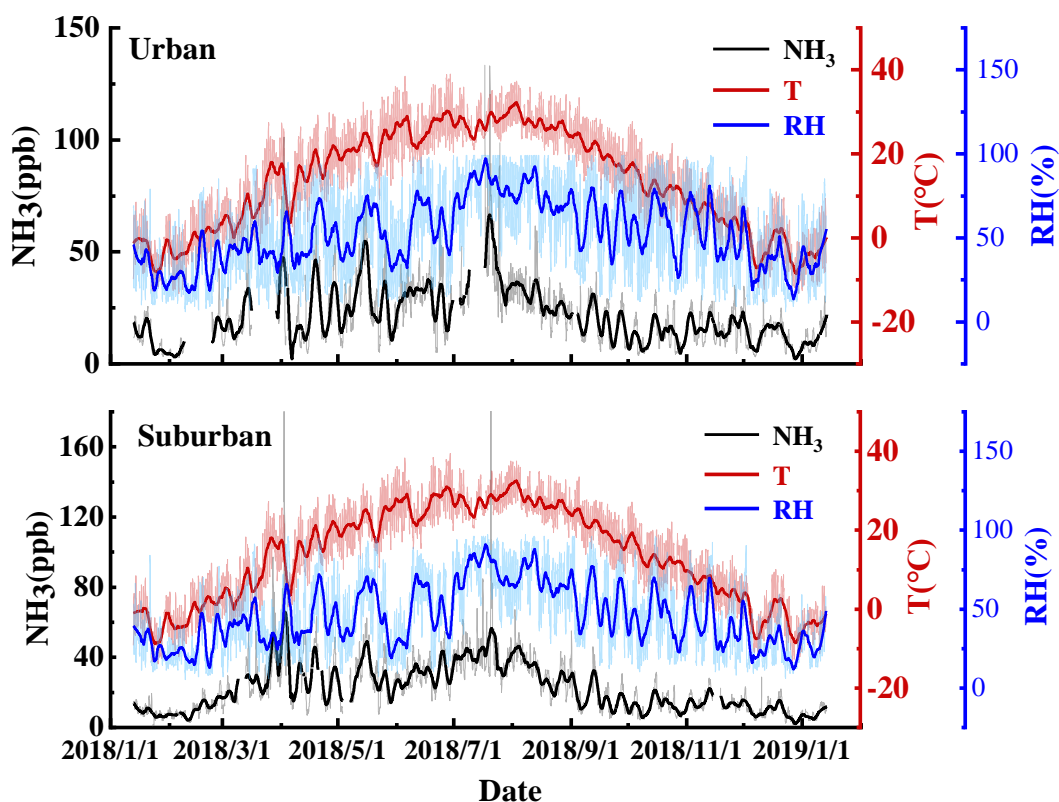
131 Totally, 7645 and 8342 valid hourly mean observations were obtained for the urban (Haidian) and  
132 suburban (Changping) sites, respectively. In addition, the urban and suburban meteorological data  
133 (temperature, relative humidity, wind direction, and wind speed) during the sampling period were  
134 obtained from the Haidian Meteorological Observation Station and Changping Meteorological Station,  
135 respectively.

### 136 **3. Results and discussion**

#### 137 *3.1. Overall variations in the NH<sub>3</sub> mixing ratios*

138 Fig. 2 displays the time-series variations in the NH<sub>3</sub> mixing ratios, temperatures, and relative

139 humidity at the urban and suburban sites in Beijing. At the urban site, the mean  $\pm 1\sigma$ , median, maximum,  
 140 and minimum values of the hourly average  $\text{NH}_3$  mixing ratio during the observation period were  $21 \pm 14$   
 141 ppb, 17 ppb, 133 ppb and 1.6 ppb, respectively. At the suburban site, the corresponding values were  $22$   
 142  $\pm 15$  ppb, 18 ppb, 199 ppb, and 0.8 ppb, respectively. The annual average and range of the  $\text{NH}_3$  mixing  
 143 ratio at the suburban site were marginally higher than those at the urban site. The characteristics of the  
 144 weekly smoothed data indicate that the  $\text{NH}_3$  variations and temperature/humidity fluctuations at the two  
 145 sites were practically consistent, which suggests that both sites were under the influence of similar  
 146 weather systems. The hourly mean  $\text{NH}_3$  concentrations at the urban site were significantly correlated ( $R$   
 147  $= 0.849, P < 0.01$ ) with those at the suburban site.



148  
 149 Fig. 2. Temporal variations in the hourly average  $\text{NH}_3$  mixing ratios, temperatures ( $T$ ) and relative humidity ( $RH$ ) at the urban and suburban  
 150 stations in Beijing. Continuous thick lines were smoothed with 168 points (7 days) by using the Savitzky–Golay method.

151

152 Table 1 shows the comparison of atmospheric  $\text{NH}_3$  concentrations (ppb) observed in different areas.



153 Meng et al. (2011) obtained an average NH<sub>3</sub> mixing ratio of  $22.8 \pm 16.3$  ppb for the period 2008-2010 in  
 154 Beijing urban area, which is very close to our result ( $21 \pm 14$  ppb) for 2018-2019. Therefore, the annual  
 155 average NH<sub>3</sub> mixing ratio in urban Beijing did not change significantly from 2008 to 2019. Moreover,  
 156 results from this study and Meng et al. (2011) indicate that the NH<sub>3</sub> concentrations at the urban and  
 157 suburban sites were higher than those in the background areas. The observed NH<sub>3</sub> concentrations in  
 158 Beijing were higher than those in northwest China (Meng et al., 2010) and the Yangtze River Delta region  
 159 (Chang et al., 2019). The average annual NH<sub>3</sub> concentration in the urban area of Shanghai, a mega city  
 160 in the Southeast China (31° N), was approximately 50% lower than that in urban Beijing. This might be  
 161 related to the fact that the North China Plain, in which Beijing is located, is one of the most intensive  
 162 agricultural production regions in China. The differences in the soil properties of Beijing and Shanghai  
 163 may be another reason because the loss of soil NH<sub>3</sub> can increase with an increase in the soil pH (Ju et al.,  
 164 2009). Shanghai and its surrounding areas are dominated by acidic soil of paddy fields (Zhao et al., 2009),  
 165 whereas Beijing is dominated by the alkaline soils of dry land (Wei et al., 2013). In addition, the climate  
 166 in Beijing is much drier than in Shanghai so that less atmospheric NH<sub>3</sub> in Beijing can be removed than  
 167 in Shanghai by wet deposition.

168 **Table 1.** Comparison of the atmospheric NH<sub>3</sub> concentrations (ppb) observed in different areas.

Period	Location	Methodology	Types	Concentration	Reference
2018.01-2019.01	Beijing, CN	Online monitor	Urban	20.8±13.7	This study
			Suburban	21.9±14.9	
2008.02-2010.07	Beijing, CN	Passive sampler	Urban	22.8±16.3	Meng et al., 2011
2007.01-2010.07			Background	10.2±10.8	
2014.5-2015.6	Shanghai, CN	Passive sampler	Urban	7.8	Chang et al. 2019
			Suburban	6.8	
2006.04-2007.04	Xi'an, CN	Passive sampler	Urban	18.6	Cao et al. 2009
			Suburban	20.3	
2017.12-2018.2	Hebei, CN	Online monitor	Rural	16.7±19.7	He et al. 2020
2008	Qinghai, CN	Passive sampler	Rural	4.1±2.2	Meng et al. 2010

2003.7-2011.9	Toronto, CA	Passive sampler	Urban	2.3-3.0	Hu et al. 2014
			Rural	0.1-4	
2016.4-2017.10	New York, US	Active and passive system	Urban	2.2-3.2	Zhou et al. 2019
			Rural	0.6-0.8	
2017.12	Tokyo, JP	semi-continuous microflow analytical system	Urban	4.1	Osada et al. 2019
2013.1-2015.12	Delhi, IN	Automatic analyzer	Urban	53.4±14.9	Saraswati et al., 2019
2012.10-2013.9	Jaunpur, IN	Glass flask sampling	Suburban	51.6±22.8	Singh and Kulshrestha, 2014
2008.1-2009.2	Bamako, MLI	Passive sampler	Urban	46.7	Adon et al., 2016
2006.3-2017.4	Edmonton, CA	Online monitor	Urban	2.4±0.6	Yao et al., 2016
2010.9-2011.8	Seoul, KR	Online monitor	Urban	10.9±4.25	Phan et al., 2013
2004.3-2004.7	Munster, DE	Wet denuder	Urban	5.2	Vogt et al., 2005

169

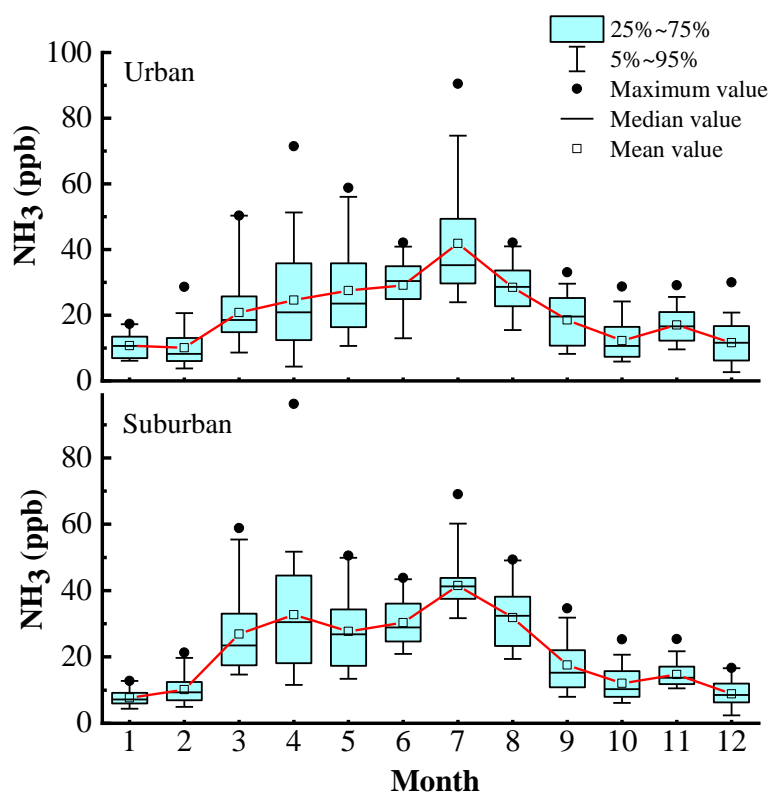
170 Table 1 also shows observational results of atmospheric NH<sub>3</sub> from some other countries. The NH<sub>3</sub>  
171 mixing ratios in the United States (Edgerton et al., 2007; Nowak et al., 2006; Zhou et al. 2019), Scotland  
172 (Burkhardt et al., 1998), Canada (Hu et al., 2014), Japan (Osada et al., 2019), and Germany (Vogt et al.,  
173 2005) were 0.23–13 ppb, 1.6–2.3 ppb, 0.1–4 ppb, 4.1 ppb, and 5.2 ppb, respectively. These values are  
174 considerably lower than those in Beijing. However, Delhi, India (Saraswati et al., 2019), exhibited higher  
175 NH<sub>3</sub> mixing ratio (53.4±14.9 ppb) than Beijing did. This result might be attributed to the well-developed  
176 livestock breeding activities in Delhi. This comparison indicates that in the decade before 2019, the NH<sub>3</sub>  
177 concentration in Beijing did not change considerably, but it is of the highest in big cities in China and  
178 much higher than those observed in developed countries in America, Europe and Asia.

### 179 3.2. Seasonal variations

180 Fig. 3 displays the monthly statistics for the NH<sub>3</sub> mixing ratios at the urban and suburban sites in  
181 Beijing. The seasonal variations in the NH<sub>3</sub> mixing ratios were very similar at the urban and suburban  
182 sites, with higher mixing ratios in the spring and summer and low ones in the autumn and winter. The  
183 daily mean concentrations fluctuated considerably in the spring, particularly in April. The highest mean

184  $\text{NH}_3$  concentrations at the urban and suburban sites were  $42 \pm 17$  ppb and  $42 \pm 8.2$  ppb, respectively. Both  
185 occurred in July, when the  $\text{NH}_3$  concentrations fluctuated considerably as well. On average, the seasonal  
186  $\text{NH}_3$  mixing ratios at the urban and suburban sites can be arranged as follows: summer > spring > autumn >  
187 winter. The main grain crops in the rural area of Beijing are corn and wheat. Corn is categorized as spring  
188 corn and summer corn, which are sown in April and June, respectively. Usually, a large amount of base  
189 fertilizer is applied when planting corn and the topdressing after 2 months. Wheat is sown from  
190 September to October, and the topdressing is applied in the following spring. The volatilization of  
191 nitrogen fertilizers can cause an increase in atmospheric  $\text{NH}_3$  mixing ratios and its fluctuations in  
192 fertilization seasons (Zhang et al., 2016). In addition, the high temperature in summer should also be  
193 responsible to the high  $\text{NH}_3$  mixing ratios in this season. An increase in the temperature can increase the  
194 biological activity and thus enhance the  $\text{NH}_3$  production and emission. High temperature is also  
195 conducive for the volatilization of the urea and diammonium phosphate applied to crops. Moreover, the  
196 equilibrium among ammonium nitrate particles, gaseous  $\text{NH}_3$ , and nitric acid is transferred to the gas  
197 phase at high temperature, which increases the  $\text{NH}_3$  concentration (Behera et al., 2013). Sewage treatment,  
198 household garbage, golf courses, and human excreta are crucial  $\text{NH}_3$  sources that are easily neglected  
199 (Pu et al., 2020). The relatively low  $\text{NH}_3$  concentrations in the autumn and winter might be caused by the  
200 decrease in  $\text{NH}_3$  emission in the soil and vegetation, the decrease in the  $\text{NH}_4\text{NO}_3$  decomposition capacity  
201 at low temperatures, and the reduced human activities caused by a large floating population returning to  
202 their native locations outside Beijing during the Spring Festival (Liao et al., 2014). In the spring and  
203 summer, the  $\text{NH}_3$  mixing ratios at the suburban site were higher than those at the urban site, which might  
204 be related to the higher agricultural activity around the suburban site. In the autumn and winter, the  $\text{NH}_3$   
205 mixing ratios at the urban site were marginally higher than those at the suburban site. In the autumn and

206 winter seasons, the influences of agricultural activities on the NH<sub>3</sub> concentration were weakened,  
 207 whereas the influences of other sources (such as traffic sources) were enhanced. According to Wang et  
 208 al. (2019), the traffic NH<sub>3</sub> emission per unit area in Haidian (urban site) was three times higher than that  
 209 in Changping (suburban site). This difference in traffic source emissions might have resulted in higher  
 210 NH<sub>3</sub> concentrations at the urban site than at the suburban site in the autumn and winter.



211

212

Fig. 3. Monthly statistical variation in the NH<sub>3</sub> mixing ratios at the urban and suburban sites in Beijing.

213

214

Table 2. NH<sub>3</sub> mixing ratios (ppb) measured at the urban and suburban sites in Beijing.

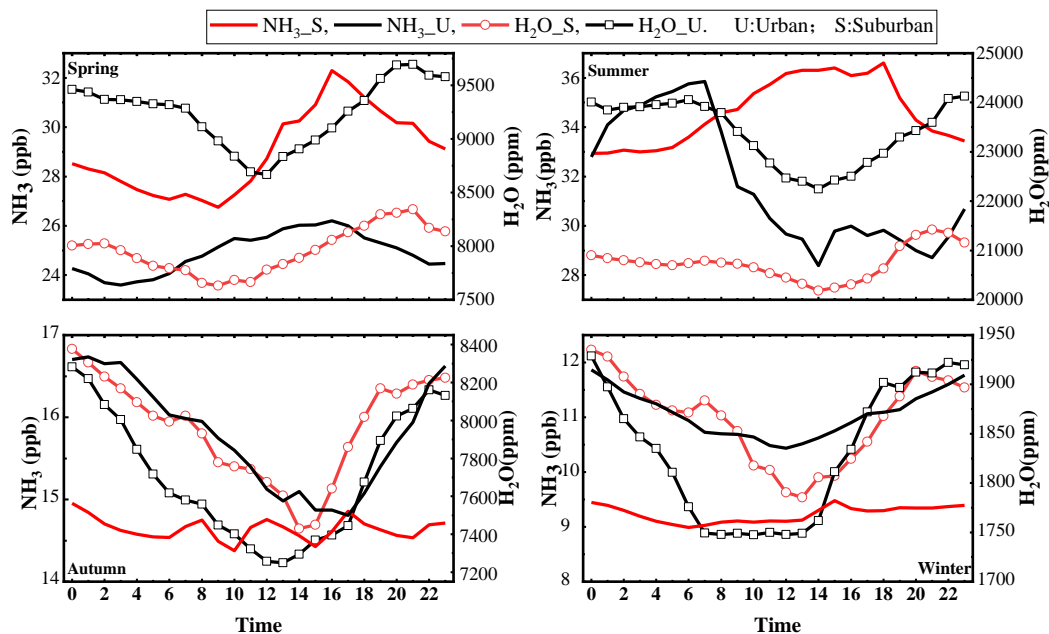
Site	Time period	Mean	Standard deviation	Minimum	Median	Maximum
Urban	Annual	21	14	1.6	17	133
	Spring	25	16	1.9	21	101
	Summer	32	12	5.0	30	133
	Autumn	16	7.5	3.8	15	41

	Winter	11	6.7	1.6	9.9	42
	Annual	22	15	0.8	18	198
	Spring	29	16	6.8	26	180
Suburban	Summer	35	12	12.1	33	199
	Autumn	15	6.8	4.1	13	55
	Winter	9.2	4.5	0.8	8.4	29

215

### 216 3.3. Diurnal variations

217 Figure 4 displays the average diurnal variations in the  $\text{NH}_3$  and  $\text{H}_2\text{O}$  mixing ratios in different  
 218 seasons at the urban and suburban sites in Beijing. Ambient  $\text{NH}_3$  exhibited different diurnal behaviors in  
 219 different seasons.



220

221 Fig. 4. Average diurnal variations in the  $\text{NH}_3$  and  $\text{H}_2\text{O}$  mixing ratios in different seasons at the urban and suburban sites in Beijing.

222

223 In spring, the average diurnal variations in the  $\text{NH}_3$  mixing ratio were similar at the urban and  
 224 suburban sites. The diurnal variations exhibited a single-peak pattern with high values in the daytime and  
 225 low values at night. The  $\text{NH}_3$  mixing ratio began to increase in the morning, reached its maximum value

226 at 16:00, and then decreased gradually. The lowest mixing ratios at the urban and suburban sites occurred  
227 at 03:00 and 09:00, respectively. The  $\text{NH}_3$  mixing ratio began to increase earlier at the urban site than at  
228 the suburban site. A plausible explanation to the earlier increase in the  $\text{NH}_3$  emission at the urban site is  
229 the traffic emission in the morning rush hours. In spring, the mixing ratio of  $\text{NH}_3$  was higher at the  
230 suburban site than that at the urban site, with an average difference of 4.1 ppb and a maximum difference  
231 of 6.1 ppb. The average diurnal amplitude of the  $\text{NH}_3$  mixing ratio at the suburban site was 5.3 ppb,  
232 which was higher than that (2.6 ppb) at the urban site. At the urban site, the average diurnal variations in  
233 the  $\text{NH}_3$  and  $\text{H}_2\text{O}$  mixing ratios exhibited nearly opposite trends. The  $\text{H}_2\text{O}$  mixing ratio had high values  
234 in the night and low values in the day. At the suburban site, the variation characteristics of  $\text{NH}_3$  and  $\text{H}_2\text{O}$   
235 were very similar; however, the peak  $\text{NH}_3$  concentration occurred 5 hours earlier than the peak  $\text{H}_2\text{O}$   
236 concentration. In spring, in contrast to the  $\text{NH}_3$  mixing ratio, the  $\text{H}_2\text{O}$  mixing ratio at the urban site was  
237 1279 ppm higher than that at the suburban site.

238 The diurnal variation in the  $\text{NH}_3$  mixing ratio at the suburban site in summer was similar to that in  
239 spring. This phenomenon was also observed in the rural areas of Shanghai by Chang et al. (2019). The  
240 diurnal variations of  $\text{NH}_3$  at the suburban site were considerably affected by the temperature and the  
241 contribution from volatile  $\text{NH}_3$  sources. However, the diurnal summer variation of  $\text{NH}_3$  at the urban site  
242 was completely different from that at the suburban site. The summer level of  $\text{NH}_3$  at the urban site was  
243 obviously lower during the daytime and evening than that at the suburban site, increased gradually from  
244 21:00 to levels higher its suburban counterpart, dropped after reaching its peak value at 7:00, and then  
245 reached its lowest value at 14:00. The diurnal pattern (with a peak in early morning) has been observed  
246 in other areas, such as rural (Ellis et al., 2011), urban (Gong et al., 2011), and steppe areas located far  
247 away from human activity (Wentworth et al., 2016). Kuang et al. (2020) believed that such diurnal pattern

248 of  $\text{NH}_3$  was caused by the evaporation of dew in the morning, which resulted in the release of  $\text{NH}_3$   
249 originally stored in the droplets. A lag was observed between the changes in the  $\text{NH}_3$  and  $\text{H}_2\text{O}$   
250 concentrations in the early morning, which supported the hypothesis of Kuang et al (2020). In addition,  
251 the increase in the  $\text{NH}_3$  concentration in the morning might have been caused by the breakup of the  
252 boundary layer formed at night. The downward mixing of air with a higher  $\text{NH}_3$  concentration in the  
253 residual layer led to a morning increase in the  $\text{NH}_3$  concentration on the ground (Bash et al., 2010). In  
254 summer, the  $\text{NH}_3$  concentrations at the suburban site were significantly higher than those at the urban  
255 site during the daytime and first half of the night. The average diurnal amplitude of the  $\text{NH}_3$  concentration  
256 was 7.5 ppb and 3.7 ppb at the urban and suburban sites, respectively. Similar to the situation in spring,  
257 the  $\text{H}_2\text{O}$  concentrations at the urban site were significantly higher than those at the suburban site in the  
258 summer.

259 In autumn, the  $\text{NH}_3$  concentration at the suburban site was relatively stable and remained nearly all  
260 the time lower than that at the urban site, which showed low values during the day and high values during  
261 the night, with a peak at midnight and a minimum (about 2.0 ppb lower than the peak) at 17:00. The  $\text{H}_2\text{O}$   
262 concentration was marginally lower (250 ppm) at the urban site than at the suburban site. The diurnal  
263 profiles of  $\text{H}_2\text{O}$  at both sites resemble that of  $\text{NH}_3$  at the urban site, but the lowest values of  $\text{H}_2\text{O}$  occurred  
264 earlier than the lowest value of  $\text{NH}_3$  at the urban site.

265 The diurnal patterns of  $\text{NH}_3$  and  $\text{H}_2\text{O}$  in winter were similar to those in autumn though the mixing  
266 ratios of  $\text{NH}_3$  and  $\text{H}_2\text{O}$  were lower than their autumn counterparts. There were two slight differences: (1)  
267 the mixing ratios of  $\text{NH}_3$  at both sites exhibited lower fluctuations than those in autumn and (2) the  
268 mixing ratio of  $\text{NH}_3$  at the urban site reached its minimum in winter earlier than that in autumn.

269 The above results indicate that although the two sites were under the influence of similar weather

270 systems, the diurnal variations in the NH<sub>3</sub> mixing ratios at the two sites were different in different seasons.  
 271 This finding suggests that different NH<sub>3</sub> sources and possibly sinks had different contributions to the NH<sub>3</sub>  
 272 concentrations at the urban and suburban sites. Additional studies should be conducted to better  
 273 understand the behaviors of atmospheric NH<sub>3</sub> and its influencing factors.

#### 274 3.4. Effect of meteorological factors on the NH<sub>3</sub> levels

275 Table 3 presents the annual and seasonal correlation coefficients between the daily means of NH<sub>3</sub>  
 276 mixing ratios and those of the temperature, relative humidity, and wind speed at the two sites. Annually,  
 277 the NH<sub>3</sub> mixing ratios at both sites were positively correlated with temperature and relative humidity and  
 278 negatively correlated with wind speed, and the correlations are all highly significant. However, the  
 279 correlations deteriorated somewhat in warm seasons. In summer and autumn, no significant correlations  
 280 were noted between ambient NH<sub>3</sub> and temperature at the two sites. The correlation between NH<sub>3</sub> and  
 281 wind speed in summer was much weaker than in the other seasons. The relative humidity was stronger  
 282 correlated with the NH<sub>3</sub> concentration at the two sites than temperature, which can be perceived in Fig 2.  
 283 Also, the correlation between NH<sub>3</sub> and relative humidity did not vary much from season to season. This  
 284 implies a possibility that relative humidity exerts a certain influence on the variation of the NH<sub>3</sub> level in  
 285 the surface layer.

286

287 Table 3. Correlations between the daily mean values of NH<sub>3</sub> and meteorological elements (Spearman's  
 288 rank correlation coefficient)

Site	Time Period	Temperature	Relative humidity	Wind speed
Urban	Annual	0.680**	0.706**	-0.370**
	Spring	0.450**	0.645**	-0.540**
	Summer	0.043	0.488**	-0.106**
	Autumn	0.101	0.759**	-0.413**
	Winter	0.596**	0.690**	-0.449**



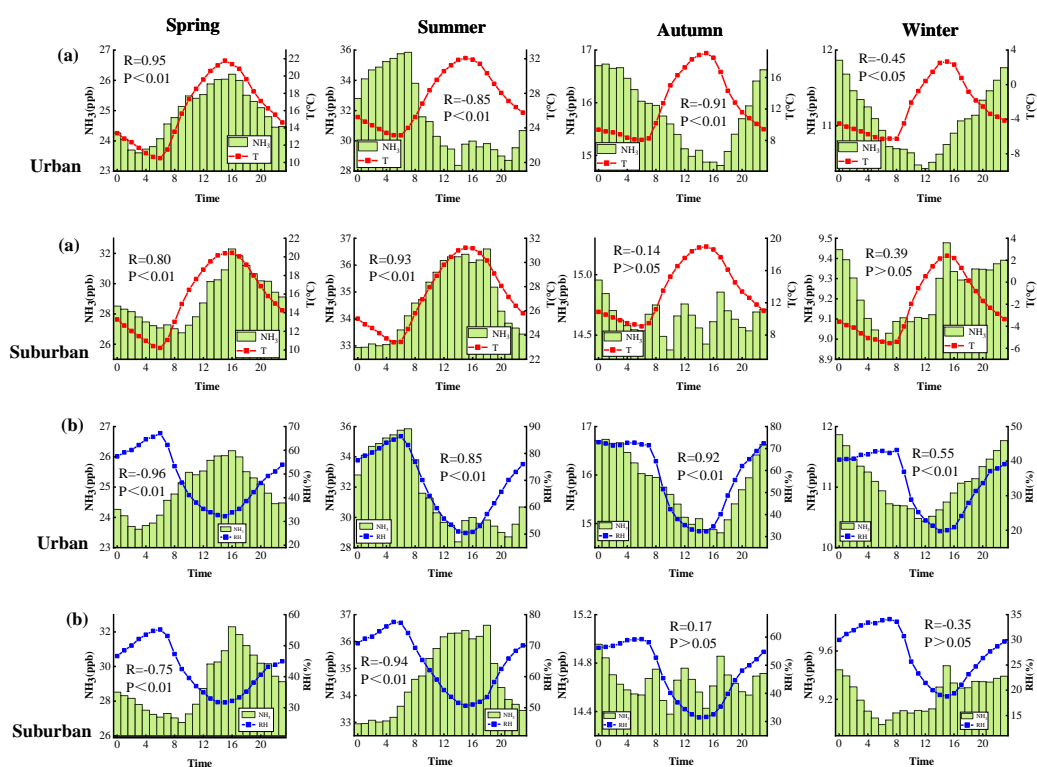
	Annual	0.745**	0.730**	-0.325**
	Spring	0.256*	0.518**	-0.391**
Suburban	Summer	0.126	0.576**	-0.061**
	Autumn	0.135	0.792**	-0.618**
	Winter	0.676**	0.663**	-0.545**

289 \*: at the 0.05 significant level; \*\*: at the 0.01 significant level.

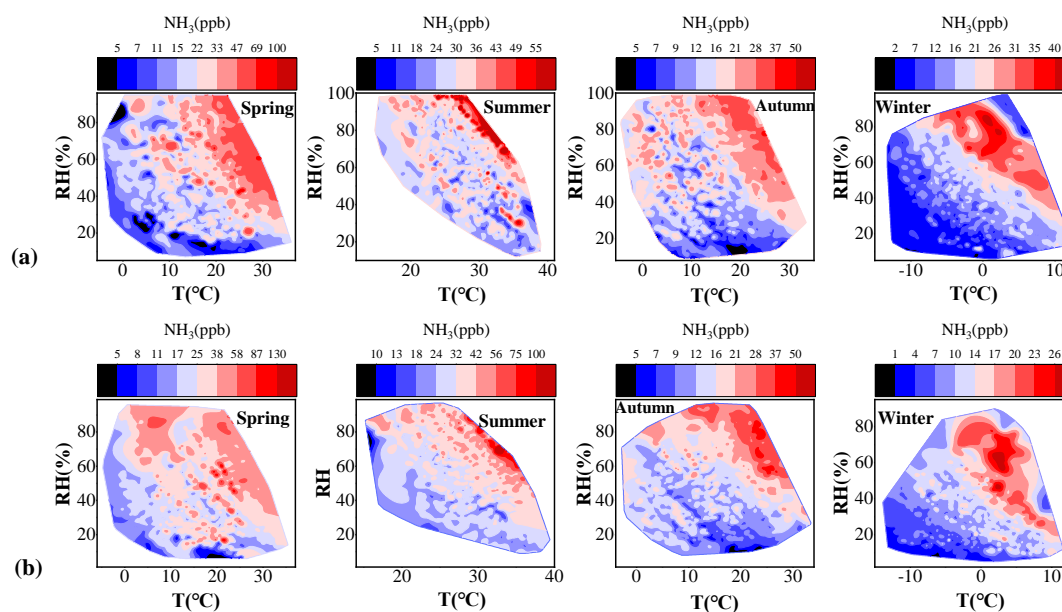
290

291 Fig. 5 displays the seasonal mean diurnal variations in the NH<sub>3</sub> mixing ratio, temperature, and  
 292 relative humidity in different seasons at the urban and suburban sites, with their correlation coefficients  
 293 shown in Fig. S5. At the urban site, the seasonal-hourly means of the NH<sub>3</sub> mixing ratio were positively  
 294 (negatively) correlated with those of temperature (relative humidity) in spring, but the correlations were  
 295 reversed in the other seasons. At the suburban site, the seasonal-hourly means of the NH<sub>3</sub> mixing ratio  
 296 were positively (negatively) correlated with those of temperature (relative humidity) in the spring and  
 297 summer, but less correlated in autumn and winter. Similar correlation behaviors (diurnal variations) were  
 298 found at both sites in spring, but in other seasons the correlations (diurnal variations) at the urban site  
 299 behaved differently from those at the suburban site. The inconsistent behaviors in summer, autumn and  
 300 winter caused urban-suburban differences in the annual-diurnal patterns of NH<sub>3</sub>, temperature and relative  
 301 humidity as well as the NH<sub>3</sub>-temperature (relative humidity) correlations, as can be seen in Fig. S6.  
 302 Figure 6 displays the contour maps of the NH<sub>3</sub> mixing ratio, temperature, and relative humidity in  
 303 different seasons at the urban and suburban sites. The annual contour maps are shown in Fig. S7. As  
 304 shown in these contour maps, the NH<sub>3</sub> mixing ratios at both sites increased with relative humidity at  
 305 same temperature and increased with temperature at same relative humidity. Although there are some  
 306 scatterings in the contour maps, high NH<sub>3</sub> levels are generally associated with high temperature and  
 307 humidity. In winter, when air temperature was low (< 0 °C), the NH<sub>3</sub> mixing ratios at both sites often had  
 308 low values except in high humidity (>60%). An increase in temperature caused higher NH<sub>3</sub> mixing ratios

309 at both sites; however, the  $\text{NH}_3$  concentration at the suburban site was more significantly correlated with  
 310 temperature than that at the urban site (Table 3), suggesting that volatile  $\text{NH}_3$  sources might have a higher  
 311 contribution to the  $\text{NH}_3$  concentration in suburban than in urban area. A higher amount of  $\text{NH}_3$  removal  
 312 through chemical transformation is expected during the day at the urban site than at the suburban site  
 313 because the urban area had higher relative humidity and amounts of particulate matters, and higher  
 314 emissions of acid gases (particularly  $\text{NO}_x$ ) than the suburban area. In 2018, the concentrations of  $\text{PM}_{2.5}$ ,  
 315  $\text{SO}_2$  and  $\text{NO}_2$  were  $50 \mu\text{g}/\text{m}^3$ ,  $5 \mu\text{g}/\text{m}^3$ ,  $43 \mu\text{g}/\text{m}^3$  in Haidian, and  $46 \mu\text{g}/\text{m}^3$ ,  $6 \mu\text{g}/\text{m}^3$ ,  $35 \mu\text{g}/\text{m}^3$  in  
 316 Changping, respectively, as reported by Beijing Ecology and Environment Statement.  
 317



318  
 319 **Fig. 5.** Diurnal variations in and correlation coefficients between the  $\text{NH}_3$  mixing ratios and temperature (a), relative humidity (b) in  
 320 different seasons at the urban and suburban sites in Beijing.



321

322 Fig. 6. Contour maps of the  $\text{NH}_3$  mixing ratio, temperature, and relative humidity in different seasons at the urban and suburban sites in

323 Beijing (a: Urban, b: Suburban).

324

325 To explore the influence of wind on the  $\text{NH}_3$  mixing ratios, rose charts were drawn for the hourly

326 mean concentration of  $\text{NH}_3$ , wind direction frequency, and wind speed during the observation period (Fig.

327 7). The large-scale wind circulation in the North China Plain is often influenced by the mountain-plain

328 topography; therefore, the dominant winds in this region are southerly (from noon to midnight) and

329 northerly (from midnight to noon) (Lin et al., 2009; Lin et al., 2011). As displayed in Fig. 7, some

330 differences existed in the distributions of the surface wind between the urban and suburban sites. The

331 prevailing surface winds were northeasterly and southwesterly at the urban site and northwesterly and

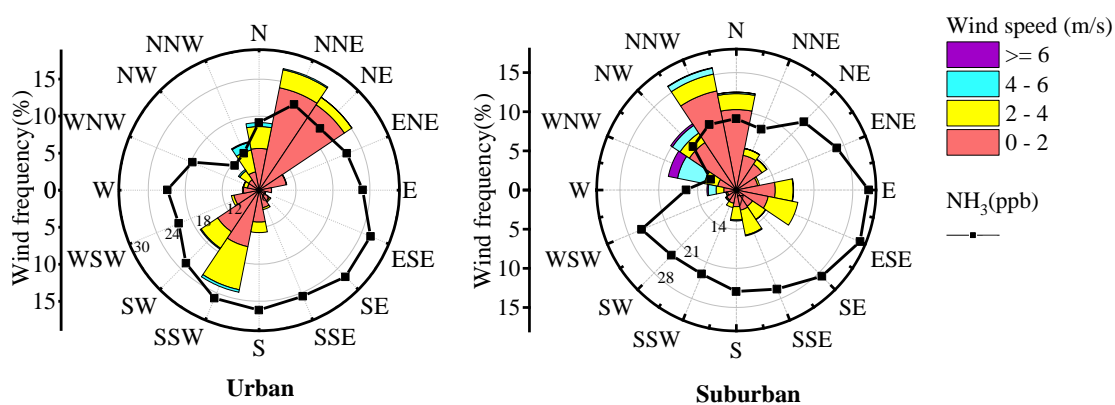
332 easterly at the suburban site. At the urban site, the  $\text{NH}_3$  mixing ratios were relatively high when the winds

333 originated from the southern sectors and relatively low when the winds originated from the northwest

334 sectors. Therefore, under southwest wind, air masses from the south of Beijing carry not only air

335 pollutants but also higher levels of  $\text{NH}_3$  to the urban site. Meng et al. (2017) examined the effect of long-

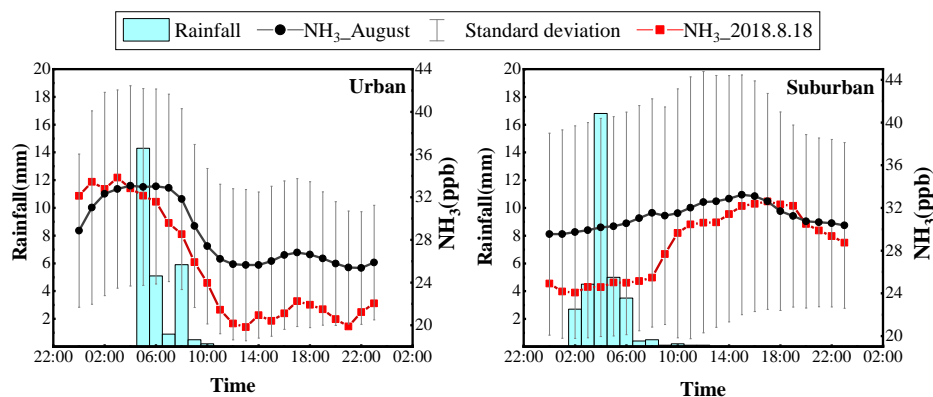
336 range air transport on the urban  $\text{NH}_3$  levels in Beijing during the summer through trajectory analysis.  
 337 They concluded that the air mass from the southeast has a cumulative effect on the  $\text{NH}_3$  concentration.  
 338 Although the dominant wind direction at the suburban site was different from that at the urban site, the  
 339  $\text{NH}_3$  mixing ratios were also relatively high in the south sectors. Thus, winds from the southeast, south,  
 340 and southwest can elevate levels of atmospheric  $\text{NH}_3$  at both the urban and suburban sites. The  $\text{NH}_3$   
 341 mixing ratios were relatively low when air masses originated from the northwest sector at urban site and  
 342 from the west sector at the suburban site. The west and northwest winds were stronger and promoted the  
 343 dilution and diffusion of  $\text{NH}_3$  emitted into the boundary layer.



344 **Urban** **Suburban**  
 345 Fig. 7. Rose maps of the  $\text{NH}_3$  mixing ratios, wind frequency, and wind speed in different wind direction sectors.

346  
 347 As a water-soluble gas,  $\text{NH}_3$  can be impacted by precipitation. Heavy rainfall occurred on August  
 348 18, 2018 (Fig. 8). Before the rainfall, the  $\text{NH}_3$  concentration at the urban site was higher than the average  
 349 level in August. After the rainfall, the  $\text{NH}_3$  concentration decreased rapidly, and it was significantly lower  
 350 than the mean value in August. However, the diurnal pattern of  $\text{NH}_3$  on that day did not differ  
 351 considerably from the average diurnal pattern in August. On the same day, the  $\text{NH}_3$  mixing ratio at the  
 352 suburban site remained at a low level during the rainfall period, which was considerably lower than the  
 353 August mean  $\text{NH}_3$  concentration during the same time of day. However, the  $\text{NH}_3$  mixing ratio increased

354 rapidly after the precipitation and reached the mean level at 17:00. The rainfall might have an obvious  
 355 clearing effect on NH<sub>3</sub> but more case studies are needed to reach a robust conclusion.



356  
 357 **Fig. 8.** Diurnal variations in the rainfall and NH<sub>3</sub> concentration on August 18, 2018.

358

#### 359 4. Conclusions

360 In this study, the atmospheric NH<sub>3</sub> concentrations at an urban site and a suburban site in Beijing  
 361 were continuously and simultaneously observed from January 2018 to January 2019. The mean NH<sub>3</sub>  
 362 mixing ratios were  $21 \pm 14$  ppb and  $22 \pm 15$  ppb at the urban and suburban sites, respectively. These NH<sub>3</sub>  
 363 levels are among the highest mean values found in China and much higher than those reported for some  
 364 developed countries in America, Europe and Asia. In the summer and spring, the NH<sub>3</sub> mixing ratios at  
 365 the suburban site were slightly higher than those at the urban site. In the autumn and winter, however,  
 366 the situation was reversed. The highest NH<sub>3</sub> mixing ratios at the urban and suburban sites were all found  
 367 in July. The lowest NH<sub>3</sub> mixing ratio occurred in February at the urban site and in January at the suburban  
 368 site. A comparison with data from literature shows that the mean concentration of NH<sub>3</sub> in Beijing did not  
 369 change considerably in the decade before 2019.

370 The hourly mean NH<sub>3</sub> mixing ratios at the urban site were highly correlated ( $R = 0.849$ ,  $P < 0.01$ )  
 371 with those at the suburban site. However, the mean diurnal variations in the NH<sub>3</sub> mixing ratios at the

372 urban and suburban sites were different. At the urban site, lower NH<sub>3</sub> mixing ratios were observed in the  
373 daytime and higher ones at night. The opposite trend was observed at the suburban site. Although both  
374 sites were under the influence of similar weather systems, the seasonal-diurnal variations in the NH<sub>3</sub>  
375 mixing ratio were different at the urban and suburban sites, suggesting that NH<sub>3</sub> sources had different  
376 relative contributions to the NH<sub>3</sub> levels at the urban and suburban sites.

377 The relationship of meteorological factors with the NH<sub>3</sub> mixing ratio was complex. Overall, the NH<sub>3</sub>  
378 mixing ratios increased with relative humidity and temperature at both sites. Relative humidity was stronger  
379 correlated with the NH<sub>3</sub> mixing ratio at both sites. The situation in different seasons varied and was site-  
380 dependent, which warrants further studies. A high wind speed (mainly under northwesterly) suppressed  
381 the levels of NH<sub>3</sub> at both sites. The NH<sub>3</sub> mixing ratios were higher under southerly wind conditions.  
382 Rainfall had a certain scavenging effect on NH<sub>3</sub> but had little effect on the diurnal variations in the NH<sub>3</sub>  
383 concentration.

384

385 **Data availability.** The data of stationary measurements are available upon request to the contact author  
386 Weili Lin (linwl@muc.edu.cn).

387

388 **Author contributions.** ZL and WL developed the idea for this paper, formulated the research goals, and  
389 carried out the measurement at urban site. WP and ZM carried out the NH<sub>3</sub> field observations at the  
390 suburban site.

391

392 **Competing interests.** The authors declare that they have no conflict of interest.

393

394 **Acknowledgments.** This study was funded by the National Natural Science Foundation of China  
395 (Grant No. 91744206) and the Beijing Municipal Science and Technology (Z181100005418016).

396

397 **Reference**

398 Adon, M., Yoboué, V., Galy-Lacaux, C., Liousse, C., Diop, B., Doumbia, E. H. T., Gardrat, E., Ndiaye,  
399 S. A. and Jarnot, C.: Measurements of NO<sub>2</sub>, SO<sub>2</sub>, NH<sub>3</sub>, HNO<sub>3</sub> and O<sub>3</sub> in West African urban  
400 environments, *Atmospheric Environment*, 135, 31–40,  
401 <https://doi.org/10.1016/j.atmosenv.2016.03.050>, 2016.

402 Baer, D. S., Paul, J. B., Gupta, M. and O’Keefe, A.: Sensitive absorption measurements in the near-  
403 infrared region using off-axis integrated-cavity-output spectroscopy, *Applied Physics B: Lasers*  
404 *and Optics*, 75(2–3), 261–265, doi:10.1007/s00340-002-0971-z, 2002.

405 Baer, D., Gupta, M., Leen, J. B., and Berman, E.: Environmental and atmospheric monitoring using  
406 off-axis integrated cavity output spectroscopy (OA-ICOS). *American laboratory*, 44(10), 20–23,  
407 2012.

408 Bash, J. O., Walker, J. T., Katul, G. G., Iones, M. R., Nemitz, E. and Robarge, W. P.: Estimation of in-  
409 canony ammonia sources and sinks in a fertilized zea mays field, *Environmental Science and*  
410 *Technology*, 44(5), 1683-1689, doi:10.1021/es9037269, 2010.

411 Behera, S. N., Sharma, M., Aneja, V. P. and Balasubramanian, R.: Ammonia in the atmosphere: A  
412 review on emission sources, atmospheric chemistry and deposition on terrestrial bodies,  
413 *Environmental Science and Pollution Research*, 20(11), 8092–8131, doi:10.1007/s11356-013-  
414 2051-9, 2013.

415 Burkhardt, J., Sutton, M. A., Milford, C., Storeton-West, R. L. and Fowler, D.: Ammonia

416 concentrations at a site in southern Scotland from 2 yr of continuous measurements, in  
417 *Atmospheric Environment*, 32(3), 325–331, [https://doi.org/10.1016/S1352-2310\(97\)00198-2](https://doi.org/10.1016/S1352-2310(97)00198-2).

418 Cao, J.-J., Zhang, T., Chow, J. C., Watson, J. G., Wu, F. and Li, H.: Characterization of Atmospheric  
419 Ammonia over Xi'an, China, *Aerosol Air Qual. Res.*, 9(2), 277–289,  
420 <https://doi.org/10.4209/aaqr.2008.10.0043>, 2009.

421 Chang, Y., Liu, X., Deng, C., Dore, A. J. and Zhuang, G.: Source apportionment of atmospheric  
422 ammonia before, during, and after the 2014 APEC summit in Beijing using stable nitrogen isotope  
423 signatures, *Atmospheric Chemistry and Physics*, 16(18), doi:10.5194/acp-16-11635-2016, 2016a.

424 Chang, Y., Zou, Z., Deng, C., Huang, K., Collett, J. L., Lin, J. and Zhuang, G.: The importance of  
425 vehicle emissions as a source of atmospheric ammonia in the megacity of Shanghai, *Atmospheric  
426 Chemistry and Physics*, 16(5), 3577-3594, doi:10.5194/acp-16-3577-2016, 2016b.

427 Chang, Y., Zou, Z., Zhang, Y., Deng, C., Hu, J., Shi, Z., Dore, A. J. and Collett, J. L.: Assessing  
428 Contributions of Agricultural and Nonagricultural Emissions to Atmospheric Ammonia in a  
429 Chinese Megacity, *Environmental Science and Technology*, 53(4), 1822–1833,  
430 doi:10.1021/acs.est.8b05984, 2019.

431 Charlson, R.J., LANGNER, J., Rodhe, H., Leovy, C.B., Warren, S.G.: Perturbation of the northern  
432 hemisphere radiative balance by backscattering from anthropogenic sulfate aerosols, *Tellus B:  
433 Chemical and Physical Meteorology*, 43(4),12, doi:10.1034/j.1600-0889.1991.t01-1-00013.x,  
434 1991.

435 Edgerton, E. S., Saylor, R. D., Hartsell, B. E., Jansen, J. J. and Alan Hansen, D.: Ammonia and  
436 ammonium measurements from the southeastern United States, *Atmospheric Environment*, 41(16),  
437 3339-3351, doi:10.1016/j.atmosenv.2006.12.034, 2007.



438 Ellis, R. A., Murphy, J. G., Markovic, M. Z., Vandenboer, T. C., Makar, P. A., Brook, J. and Mihele, C.:  
439 The influence of gas-particle partitioning and surface-atmosphere exchange on ammonia during  
440 BAQS-Met, *Atmospheric Chemistry and Physics*, 11(1), 133-145, doi:10.5194/acp-11-133-2011,  
441 2011.

442 Erisman, J. W., Bleeker, A., Galloway, J. and Sutton, M. S.: Reduced nitrogen in ecology and the  
443 environment, *Environmental Pollution*, 150(1), 140-149, doi:10.1016/j.envpol.2007.06.033, 2007.

444 Fu, X., Wang, S., Xing, J., Zhang, X., Wang, T. and Hao, J.: Increasing Ammonia Concentrations  
445 Reduce the Effectiveness of Particle Pollution Control Achieved via SO<sub>2</sub> and NO<sub>x</sub> Emissions  
446 Reduction in East China, *Environmental Science and Technology Letters*, 4(6), 221–227,  
447 doi:10.1021/acs.estlett.7b00143, 2017.

448 Ge, B., Xu, X., Ma, Z., Pan, X., Wang, Z., Lin, W., Ouyang, B., Xu, D., Lee, J., Zheng, M., Ji, D., Sun,  
449 Y., Dong, H., Squires, F.A., Fu, F., Wang, Z.: Role of ammonia on the feedback between AWC and  
450 inorganic aerosol formation during heavy pollution in the North China Plain, *Earth and Space  
451 Science*, 6, 1675-1693, <https://doi.org/10.1029/2019EA000799>, 2019.

452 Gong, L., Lewicki, R., Griffin, R. J., Flynn, J. H., Lefer, B. L. and Tittel, F. K.: Atmospheric ammonia  
453 measurements in Houston, TX using an external-cavity quantum cascade laser-based sensor,  
454 *Atmospheric Chemistry and Physics*, 11(18), 9721–9733, doi:10.5194/acp-11-9721-2011, 2011.

455 He, Y., Pan, Y., Zhang, G., Ji, D., Tian, S., Xu, X., Zhang, R. and Wang, Y.: Tracking ammonia morning  
456 peak, sources and transport with 1 Hz measurements at a rural site in North China Plain,  
457 *Atmospheric Environment*, 235, <https://doi.org/10.1016/j.atmosenv.2020.117630>, 2020.

458 Hu, Q., Zhang, L., Evans, G. J. and Yao, X.: Variability of atmospheric ammonia related to potential  
459 emission sources in downtown Toronto, Canada, *Atmospheric Environment*, 99,

460 doi:10.1016/j.atmosenv.2014.10.006, 2014.

461 Huang, X., Song, Y., Li, M., Li, J., Huo, Q., Cai, X., Zhu, T., Hu, M. and Zhang, H.: A high-resolution  
462 ammonia emission inventory in China, *Global Biogeochemical Cycles*, 26(1),  
463 doi:10.1029/2011GB004161, 2012.

464 Ju, X. T., Xing, G. X., Chen, X. P., Zhang, S. L., Zhang, L. J., Liu, X. J., Cui, Z. L., Yin, B., Christie, P.,  
465 Zhu, Z. L. and Zhang, F. S.: Reducing environmental risk by improving N management in  
466 intensive Chinese agricultural systems, *Proceedings of the National Academy of Sciences of the*  
467 *United States of America*, 106(9), 3041-3046, doi:10.1073/pnas.0813417106, 2009.

468 Krotkov, N.A., McLinden, C.A., Li, C., Lamsal, L.N., Celarier, E.A., Marchenko, S. v., Swartz, W.H.,  
469 Bucsela, E.J., Joiner, J., Duncan, B.N., Boersma, K.F., Veefkind, J.P., Levelt, P.F., Fioletov, V.E.,  
470 Dickerson, R.R., He, H., Lu, Z., Streets, D.G.: Aura OMI observations of regional SO<sub>2</sub> and NO<sub>2</sub>  
471 pollution changes from 2005 to 2015. *Atmospheric Chemistry and Physics* 16(7), 4605–4629,  
472 doi:10.5194/acp-16-4605-2016, 2016.

473 Kuang, Y., Xu, W., Lin, W., Meng, Z., Zhao, H., Ren, S., Zhang, G., Liang, L. and Xu, X.: Explosive  
474 morning growth phenomena of NH<sub>3</sub> on the North China Plain: Causes and potential impacts on  
475 aerosol formation, *Environmental Pollution*, 257, 113621, doi:10.1016/j.envpol.2019.113621,  
476 2020.

477 Liao, X., Zhang, X., Wang, Y., Liu, W., Du, J. and Zhao, L.: Comparative Analysis on Meteorological  
478 Condition for Persistent Haze Cases in Summer and Winter in Beijing, *Environmental Science*,  
479 35(06), 2031–2044, doi:10.13227/j.hjlx.2014.06.001, 2014.

480 Lin, W., Xu, X., Ge, B., Liu, X.: Gaseous pollutants in Beijing urban area during the heating period  
481 2007-2008: variability, sources, meteorological and chemical impacts, *Atmos. Chem. Phys.*, 11,

482 8157-8170, 2011.

483 Lin, W., Xu, X., Ge, B., Zhang, X.: Characteristics of gaseous pollutants at Gucheng, a rural site  
484 southwest of Beijing, *J. Geophys. Res.*, 114, D00G14, doi:10.1029/2008JD010339, 2009.

485 Meng, Z. Y., Lin, W. L., Jiang, X. M., Yan, P., Wang, Y., Zhang, Y. M., Jia, X. F. and Yu, X. L.:  
486 Characteristics of atmospheric ammonia over Beijing, China, *Atmospheric Chemistry and Physics*,  
487 11(12), 6139–6151, doi:10.5194/acp-11-6139-2011, 2011.

488 Meng, Z. Y., Xu, X. bin, Wang, T., Zhang, X. Y., Yu, X. L., Wang, S. F., Lin, W. L., Chen, Y. Z., Jiang,  
489 Y. A. and An, X. Q.: Ambient sulfur dioxide, nitrogen dioxide, and ammonia at ten background  
490 and rural sites in China during 2007–2008, *Atmospheric Environment*, 44(21–22), 2625-2631,  
491 doi:10.1016/j.atmosenv.2010.04.008, 2010.

492 Meng, Z., Lin, W., Zhang, R., Han, Z. and Jia, X.: Summertime ambient ammonia and its effects on  
493 ammonium aerosol in urban Beijing, China, *Science of the Total Environment*, 579, 1521–1530,  
494 doi:10.1016/j.scitotenv.2016.11.159, 2017.

495 Meng, Z., Wu, L., Xu, X., Xu, W., Zhang, R., Jia, X., Liang, L., Miao, Y., Cheng, H., Xie, Y., He, J. and  
496 Zhong, J.: Changes in ammonia and its effects on PM<sub>2.5</sub> chemical property in three winter seasons  
497 in Beijing, China, *Science of The Total Environment*, 749, 142208,  
498 doi:10.1016/j.scitotenv.2020.142208, 2020.

499 Nowak, J. B., Huey, L. G., Russell, A. G., Tian, D., Neuman, J. A., Orsini, D., Sjostedt, S. J., Sullivan,  
500 A. P., Tanner, D. J., Weber, R. J., Nenes, A., Edgerton, E. and Fehsenfeld, F. C.: Analysis of urban  
501 gas phase ammonia measurements from the 2002 Atlanta Aerosol Nucleation and Real-Time  
502 Characterization Experiment (ANARChE), *Journal of Geophysical Research Atmospheres*,  
503 111(17), doi:10.1029/2006JD007113, 2006.

504 Osada, K., Saito, S., Tsurumaru, H. and Hoshi, J.: Vehicular exhaust contributions to high NH<sub>3</sub> and  
505 PM<sub>2.5</sub> concentrations during winter in Tokyo, Japan, *Atmospheric Environment*, 206, 218–224,  
506 doi:10.1016/j.atmosenv.2019.03.008, 2019.

507 Pan, Y., Tian, S., Zhao, Y., Zhang, L., Zhu, X., Gao, J., Huang, W., Zhou, Y., Song, Y., Zhang, Q. and  
508 Wang, Y.: Identifying Ammonia Hotspots in China Using a National Observation Network,  
509 *Environmental Science and Technology*, 52(7), 3926–3934, doi:10.1021/acs.est.7b05235, 2018.

510 Pearson, J. and Stewart, G.R.: The deposition of atmospheric ammonia and its effects on plants, *New  
511 Phytologist*, 125(2), 283–305, doi:10.1111/j.1469-8137.1993.tb03882.x, 1993.

512 Phan, N.-T., Kim, K.-H., Shon, Z.-H., Jeon, E.-C., Jung, K. and Kim, N.-J.: Analysis of ammonia  
513 variation in the urban atmosphere, *Atmospheric Environment*, 65, 177–185,  
514 <https://doi.org/10.1016/j.atmosenv.2012.10.049>, 2013.

515 Pinder, R. W., Gilliland, A. B. and Dennis, R. L.: Environmental impact of atmospheric NH<sub>3</sub> emissions  
516 under present and future conditions in the eastern United States, *Geophysical Research Letters*,  
517 35(12), 89-90, doi:10.1029/2008GL033732, 2008.

518 Pu, W., Ma, Z., Collett, J. L., Guo, H., Lin, W., Cheng, Y., Quan, W., Li, Y., Dong, F. and He, D.:  
519 Regional transport and urban emissions are important ammonia contributors in Beijing, China,  
520 *Environmental Pollution*, 265, doi:10.1016/j.envpol.2020.115062, 2020.

521 Reay, D. S., Dentener, F., Smith, P., Grace, J. and Feely, R. A.: Global nitrogen deposition and carbon  
522 sinks, *Nature Geoscience*, 1(7), 430-437, doi:10.1038/ngeo230, 2008.

523 Saraswati, George, M. P., Sharma, S. K., Mandal, T. K. and Kotnala, R. K.: Simultaneous  
524 Measurements of Ambient NH<sub>3</sub> and Its Relationship with Other Trace Gases, PM<sub>2.5</sub> and  
525 Meteorological Parameters over Delhi, India, *Mapan - Journal of Metrology Society of India*,

526 34(1), 55–69, doi:10.1007/s12647-018-0286-0, 2019.

527 Singh, S. and Kulshrestha, U. C.: Rural versus urban gaseous inorganic reactive nitrogen in the Indo-  
528 Gangetic plains (IGP) of India, *Environ. Res. Lett.*, 9(12), 125004, <https://doi.org/10.1088/1748-9326/9/12/125004>, 2014.

529

530 UN Environment 2019. A Review of 20 Years' Air Pollution Control in Beijing. United Nations  
531 Environment Programme, Nairobi, Kenya.  
532 <https://www.unenvironment.org/resources/report/review-20-years-air-pollution-control-beijing>.

533 Van Breemen, N., Mulder, J. and Driscoll, C. T.: Acidification and alkalization of soils, *Plant and*  
534 *Soil*, 75(3), <https://doi.org/10.1007/BF02369968>, 1983.

535 Vogt, E., Held, A. and Klemm, O.: Sources and concentrations of gaseous and particulate reduced  
536 nitrogen in the city of Münster (Germany), *Atmospheric Environment*, 39(38), 7393–7402,  
537 <https://doi.org/10.1016/j.atmosenv.2005.09.012>, 2005.

538 Wang, K., Fan, S., Guo, J. and Sun, G.: Characteristics of ammonia emission from motor vehicle  
539 exhaust in Beijing, *Environmental Engineering*, 36(03), 98–101, doi:10.13205/j.hjgc.201803020,  
540 2019.

541 Warner, J. X., Dickerson, R. R., Wei, Z., Strow, L. L., Wang, Y. and Liang, Q.: Increased atmospheric  
542 ammonia over the world's major agricultural areas detected from space, *Geophysical Research*  
543 *Letters*, 44(6), 2875–2884, doi:10.1002/2016GL072305, 2017.

544 Wei, S., Dai, Y., Liu, B., Zhu, A., Duan, Q., Wu, L., Ji, D., Ye, A., Yuan, H., Zhang, Q., Chen, D., Chen,  
545 M., Chu, J., Dou, Y., Guo, J., Li, H., Li, J., Liang, L., Liang, X., Liu, H., Liu, S., Miao, C. and  
546 Zhang, Y.: A China data set of soil properties for land surface modeling, *Journal of Advances in*  
547 *Modeling Earth Systems*, 5(2), 212–224, doi:10.1002/jame.20026, 2013.

548 Wentworth, G. R., Murphy, J. G., Benedict, K. B., Bangs, E. J. and Collett, J. L.: The role of dew as a  
549 night-time reservoir and morning source for atmospheric ammonia, *Atmospheric Chemistry and*  
550 *Physics*, 16(11), 7435–7449, doi:10.5194/acp-16-7435-2016, 2016.

551 Wu, Z., Hu, M., Shao, K. and Slanina, J.: Acidic gases, NH<sub>3</sub> and secondary inorganic ions in PM<sub>10</sub>  
552 during summertime in Beijing, China and their relation to air mass history, *Chemosphere*, 76(8),  
553 doi:10.1016/j.chemosphere.2009.04.066, 2009.

554 Yao, X. and Zhang, L.: Trends in atmospheric ammonia at urban, rural, and remote sites across North  
555 America, *Atmos. Chem. Phys.*, 16(17), 11465–11475, <https://doi.org/10.5194/acp-16-11465-2016>,  
556 2016.

557 Zhang, B.: Atmospheric Distribution and Variation of NH<sub>3</sub> in Beijing, *Environmental Science and*  
558 *Management* 41(01), 119–122, 2016.

559 Zhang, S., Wag, A., Zhang, Z., Wang, J., Han, Y., Su, R. and Qu, Y.: On creating an anthropogenic  
560 ammonia emission inventory in capital Beijing, *Journal of Safety and Environment*, 16(02), 242–  
561 245, doi:10.13637/j.issn.1009–6094.2016.02.047, 2016.

562 Zhang, X., Wu, Y., Liu, X., Reis, S., Jin, J., Dragosits, U., van Damme, M., Clarisse, L., Whitburn, S.,  
563 Coheur, P. F. and Gu, B.: Ammonia emissions may be substantially underestimated in China,  
564 *Environmental Science and Technology*, 51(21), 12089–12096, doi:10.1021/acs.est.7b02171,  
565 2017.

566 Zhang, Y., Tang, A., Wang, D., Wang, Q., Benedict, K., Zhang, L., Liu, D., Li, Y., Collett Jr., J. L., Sun,  
567 Y. and Liu, X.: The vertical variability of ammonia in urban Beijing, China, *Atmospheric*  
568 *Chemistry and Physics*, 18(22), 16385–16398, doi:10.5194/acp-18-16385-2018, 2018.

569 Zhao, X., Xie, Y. X., Xiong, Z. Q., Yan, X. Y., Xing, G. X. and Zhu, Z. L.: Nitrogen fate and

570 environmental consequence in paddy soil under rice-wheat rotation in the Taihu lake region,  
571 China, *Plant and Soil*, 319(1), 225-234, doi:10.1007/s11104-008-9865-0, 2009.

572 Zhou, C., Zhou, H., Holsen, T. M., Hopke, P. K., Edgerton, E. S. and Schwab, J. J.: Ambient Ammonia  
573 Concentrations Across New York State, *Journal of Geophysical Research: Atmospheres*, 124(14),  
574 8287–8302, doi:10.1029/2019JD030380, 2019.